σ-aromaticity in the former and a decrease of (destabilizing) DS strain in the latter case.

(10) We predict "volume-delocalization" of σ-electrons in the case of cage compounds like tetrahedrane. Investigation of the energetic implications of this effect is in progress.[49]

Acknowledgment. Stimulating discussions with Professors P. v. R. Schleyer, M. J. S. Dewar, and L. C. Allen are acknowledged. All calculations have been carried out at the Rechenzentrum der Universität Köln. We thank the Deutschen Forschungsgemeinschaft and the Fonds der Chemischen Industrie for support.

Appendix

Bader and co-workers[19] have shown that molecular space can be divided into a collection of quantum-mechanically well-defined subspaces Ω with the aid of the topological properties of the total one-electron density distribution $\rho(r)$ of a molecule. These properties are made evident by those of the gradient vector field $\nabla\rho(\mathbf{r})$. The vector $\nabla\rho(\mathbf{r})$ always points into the direction of maximum increase in $\rho(\mathbf{r})$. The paths traversed by the vectors $\nabla\rho(\mathbf{r})$, the gradient paths, originate and terminate at critical points $\rho(\mathbf{r}_c)$ where $\nabla\rho(\mathbf{r}) = 0$. A critical point in the internuclear region of two bonded atoms A and B corresponds to a minimum of the path of maximum electron density (MED) linking A and B; at the same time it corresponds also to a maximum in all directions perpendicular to the MED path. The MED path is defined by exactly two gradient paths springing from $\mathbf{r}_c$ and ending at A and B. It has been termed "bond path" and the associated critical point $\mathbf{r}_c$ "bond critical point".[19]

All gradient paths terminating at the bond critical point between A and B form the zero-flux surface $S(A,B)$, through which the flux of $\nabla\rho(\mathbf{r})$ is everywhere zero:

$$\nabla\rho(\mathbf{r})\cdot\mathbf{n}(\mathbf{r}) = 0; \ \forall \mathbf{r} \in S(\mathbf{r})$$

$n(r)$ is the vector normal to $S(r)$.[19]

The surfaces S partition the space of the molecule in a unique way to yield subspaces Ω. As has been shown by Bader it is reasonable to assign a subspace Ω to the atom, the nucleus of which is embedded in Ω, and to consider Ω as the basin of the atom.[19] In this way, an atom in a molecule is defined.

With the definition of $\Omega(A)$ it is straightforward to calculate atomic expectation values $F_\Omega = \langle \hat{F}\rangle_\Omega$ where $\hat{F}$ is an appropriate operator. By summing values F_Ω over all atomic basins $\Omega(A)$ of a molecule, the molecular expectation value $F = \langle \hat{F}\rangle$ is obtained. For example, the sum of all atomic charges and energies obtained by the virial partitioning method is equal to the molecular charge and the molecular energy, respectively.

Temperature Dependence of Proton Recombination and Proton-Induced Quenching for 2-Naphtholate

J. Lee, G. W. Robinson, and M.-P. Bassez*

Contribution from the Picosecond and Quantum Radiation Laboratory, Texas Tech University, Lubbock, Texas 79409. Received May 30, 1986

Abstract: Lifetime and quantum yield measurements in aqueous solutions have been performed on the anion (RO*⁻) of electronically excited 2-naphthol (ROH*). Measurements were made at moderately low pH in order to determine the temperature dependence of the rate of proton recombination, k_{rec}, with this anion. As predicted by recently proposed absolute rate expressions for weak acid dissociation/recombination, k_{rec}^{-1} has the same temperature dependence and magnitude as the Debye (transverse) rotational relaxation time of the pure water solvent. It is also likely that the rate for the proton-quenching reaction, H⁺ + RO*⁻ → ROH (ground state), has the same temperature dependence as k_{rec}. These types of experiments are of great importance toward the fundamental understanding of ion-hydration reactions, since up to now purely theoretical considerations have indicated that it is the much shorter longitudinal relaxation time that sets the time scale for ion solvation in water.

Beginning with the classic work of Förster and Weller,[1–3] proton dissociation (dis) and recombination (rec) of the photon-initiated, moderately weak acid 2-naphthol ($pK_a^* \approx 2.7$) in aqueous solutions have been extensively studied.[4,5] Temperature-dependent measurements of the rate k_{dis} give an activation energy of $\sim$2.6 kcal mol⁻¹.[6–9] However, no information about the temperature dependence of k_{rec} is known.

A hydration model has been proposed[8] that correlates k_{dis} and k_{rec} for weak acids ($\Delta G_i^\circ \gtrsim 0$) with thermodynamic ionization enthalpies (ΔH_i°) and entropies (ΔS_i°). Absolute rate expressions were derived that give a good representation of the rate and equilibrium constant data for ground-state and photon-initiated univalent weak acids. If $\Delta H_i^\circ \geq 0$, both the enthalpy and entropy create barriers for the dissociation reaction, and $\Delta G^\ddagger_{dis} = \Delta G_i^\circ$. In contrast, no barriers stand in the way of the recombination reaction, and $\Delta G^\ddagger_{rec} = 0$ (see ref 8, section 12, case II). The rate expressions reduce to

$$k_{dis} \ (s^{-1}) = \tau_D^{-1}\Omega e^{+\Delta S_i^\circ/R} e^{-\Delta H_i^\circ/RT} \tag{1}$$

$$k_{rec} \ (M^{-1}\ s^{-1}) = \tau_D^{-1}\Omega \tag{2}$$

where reactants are at 1 M and where Ω is a steric/mobility factor introduced by Eigen and Kustin[10] and is equal to 0.45 ± 0.05 for protons from a fairly large precursor molecule such as 2-naphthol.[7,8]

* Permanent address: Institut Universitaire de Technologie, Université d'Angers, 49045 Angers, Cedex, France.

(1) Förster, Th. *Z. Electrochem.* **1950**, *54*, 531–535.
(2) Weller, A. *Z. Electrochem.* **1952**, *56*, 662–668.
(3) Weller, A. *Z. Phys. Chem. (Frankfurt am Main)* **1958**, *17*, 224–245.
(4) Laws, W. R.; Brand, L. *J. Phys. Chem.* **1979**, *83*, 795–802.
(5) Harris, C. M.; Selinger, B. K. *J. Phys. Chem.* **1980**, *84*, 891–898.
(6) Lee, J.; Griffin, R. D.; Robinson, G. W. *J. Chem. Phys.* **1985**, *82*, 4920–4925.
(7) Lee, J.; Robinson, G. W.; Webb, S. P.; Philips, L. A.; Clark, J. H. *J. Am. Chem. Soc.* **1986**, *108*, 6538–6542.
(8) Robinson, G. W.; Thistlethwaite, P. J.; Lee, J. *J. Phys. Chem.* **1986**, *90*, 4224–4233.
(9) Kishi, T.; Tanaka, J.; Kouyama, T. *Chem. Phys. Lett.* **1976**, *41*, 497–499.
(10) Eigen, M.; Kustin, K. *J. Am. Chem. Soc.* **1960**, *82*, 5952.

Table I. Temperature Effects[a]

T, °C	τ_d, ps	k_{dis},[b] ns^{-1}	k_s(obsd),[c] M^{-1} ns^{-1}	k_s(calcd),[d] M^{-1} ns^{-1}	k_{rec}, M^{-1} ns^{-1}	k_q',[f] M^{-1} ns^{-1}
0	17.9	0.07 ± 0.005	29 ± 10	36	26	10
20	9.3	0.09 ± 0.004	96 ± 11	70	51	19
25	8.1	(0.11)		80	58[e]	22
40	5.8	0.13 ± 0.007	119 ± 14	112	81	31
60	3.9	0.16 ± 0.011	157 ± 17	167	121	46
80	3.0	0.19 ± 0.011	204 ± 20	217	157	60

[a] [H$^+$] was corrected by Brönsted's kinetic activity coefficient for each temperature; τ_d values from ref 15. [b] k_0 = 0.127 (ns^{-1}), k_0' = 0.111 (ns^{-1}) for all temperatures. [c] k_s = (k_{rec} + k_q' + k_q) ≈ (k_{rec} + k_q'). [d] Calculated by multiplying τ_d^{-1} by a constant ratio, 0.65. [e] Estimated value from ref 8; this value and that for k_q' (T = 25 °C) should be compared with those from ref 5, 22 < k_{rec} < 50 and ~6 M^{-1} ns^{-1}, respectively (T ≈ 25 °C). The "picosecond" technique used here, as opposed to the "nanosecond" methods of ref 5, should improve the accuracy of these rather difficult determinations. The values of the parameters are now in fair agreement with those for 1-naphthol[22] (T ≈ 25 °C), 68 and 33 M^{-1} ns^{-1}, respectively, as would be expected from eq 2. [f] Columns 6 and 7 calculated from column 5 by using constant ratios, 0.725 and 0.275, respectively. These ratios were chosen in order to agree with the experimental value of k_{rec} at 25 °C.

Equation 2, which must be valid in order for eq 1 to hold, predicts that the only temperature dependence for the ion-recombination reaction lies in the Debye rotational time τ_D.[11] It is therefore of interest to determine k_{rec} experimentally as a function of temperature in order to determine whether or not the temperature dependence of k_{rec} is the same as the known temperature dependence of τ_D^{-1}.

Experimental Section

2-Naphthol (Aldrich) and deionized water (Fisher, HPLC grade) were used without further purification. The pHs of the aqueous solutions were adjusted to 2.96, 3.62, 3.94, and 4.67 (T ≈ 293 K) by dilution of concentrated HCl solutions (Du Pont, reagent grade). The pH values were measured with an ALTEX $\phi71$ pH meter and corrected by the Brönsted kinetic activity coefficient.[12] The concentration of 2-naphthol in each solution was maintained at ~8 × 10^{-5} M.

A detailed description of the experimental apparatus for temperature control, fluorescence quantum yield measurements, and single-photon-counting lifetime measurements has been discussed elsewhere.[6] Temperatures at 0, 20, 40, 60, and 80 °C were investigated, the temperature being controlled to within ±1 °C by a Borg-Warner LHP-150 heat pump and TC-108 controller. For single-photon counting, a mode-locked argon-ion laser (Coherent, 18-W INNOVA) operating at 68 MHz repetition rate was used to pump a dye laser (Coherent, 700). The output of the dye laser was cavity dumped (Coherent, 7210) at 11.4 MHz. The output pulse (fWHM = 15 ps) was frequency doubled to 305 nm. The emission from 2-naphtholate at 430 nm was then selected by an ISA double monochromator and collected by a fast-response photomultiplier (Amperex 2254B). Signals were processed by using a discriminator (ORTEC, 583) and a multichannel (ORTEC, 7010) and stored in a VAX 11/730 computer for future analysis. The system response function from the scattered 305-nm light gave a fWHM of 800 ± 50 ps. The instrumental profile was then used to convolute an analytical function to fit the signal profile from the sample. The χ^2 thus obtained was less than 2.0 for all fitted spectra.

Lifetimes

Because of the increase in acid strength (pK_a = 9.5, pK_a^* ≈ 2.7, at 25 °C)[5] of 2-naphthol (ROH) upon excitation, the excited state of the naphtholate ion (RO$^*{}^-$) is produced at pH < 9.5. The rate equations for the production of RO$^*{}^-$ and of the neutral excited state of 2-naphthol (ROH*) can be written as[2,3,5]

$$\frac{d[ROH^*]}{dt} =$$
$$[ROH^*]_0 - \{k_0 + k_{dis} + k_q[H^+]\}[ROH^*] + k_{rec}[H^+][RO^*{}^-]$$
(3)

$$\frac{d[RO^*{}^-]}{dt} = -\{k_0' + (k_{rec} + k_q')[H^+]\}[RO^*{}^-] + k_{dis}[ROH^*]$$
(4)

where k_0(k_0') and k_q(k_q') are, respectively, the conventional intramolecular rate constant and the proton-induced quenching rate constant for ROH* (RO$^*{}^-$). The constants k_0 and k_0' are com-
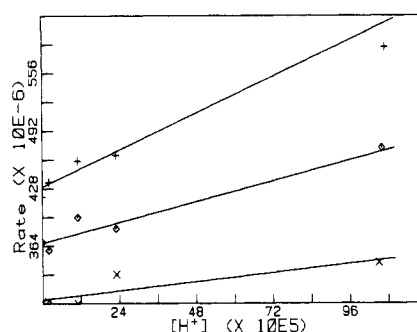
Figure 1. (λ_1 + λ_2) vs. H$^+$ concentration. ×, ◊, and + are experimental values at 0, 40, and 80 °C. The corresponding solid lines are linear least-squares fitted lines.

posed of a radiative component k_r (k_r') and a nonradiative component k_{nr} (k_{nr}'). When eq 3 and 4 are solved,[13] the time-dependent concentration of [RO$^*{}^-$] is thus

$$[RO^*{}^-] = \frac{[ROH^*]_0 k_{dis}}{\lambda_2 - \lambda_1}[e^{-\lambda_1 t} - e^{-\lambda_2 t}]$$
(5)

where

$$2\lambda_{2,1} = (a + a') \pm \{(a - a')^2 + 4k_{dis}k_{rec}[H^+]\}^{1/2}$$

and [ROH*]$_0$ is the initial (t = 0) concentration of the excited 2-naphthol. The parameters a and a' are defined as

$$a = k_0 + k_{dis} + k_q[H^+]$$

$$a' = k_0' + (k_{rec} + k_q')[H^+]$$

The expression given by eq 5 is the analytical function used in the convolution program. Hence, λ_1 and λ_2 can be obtained from the fluorescence time evolution of RO$^*{}^-$. Furthermore, since

$$\lambda_1 + \lambda_2 = (k_0 + k_0' + k_{dis}) + (k_{rec} + k_q' + k_q)[H^+]$$
(6)

plots of (λ_1 + λ_2) against [H$^+$] should yield straight lines, which can be analyzed to determine k_0 + k_0' + k_{dis} (intercepts) and k_{rec} + k_q' + k_q (slopes). Examples are shown in Figure 1 for 0, 40, and 80 °C. Parameters resulting from these fits are given in Table I for each of the five experimental temperatures. The uncertainties in the experimental parameters k_{dis} and k_s = (k_{rec} + k_q' + k_q) shown in columns 3 and 4 of Table I are obtained from the analysis of various straight lines that can be drawn through the experimental rate data. Even though the temperature-dependent intercepts (k_0 + k_0' + k_{dis}) can be more accurately assessed from previous fluorescence decay studies[6] of ROH* and RO$^*{}^-$, there is no noticeable improvement in the fitting procedure if the intercepts are fixed at these points and only the slopes allowed to vary.

(11) Hasted, J. B. *Aqueous Dielectrics*; Chapman and Hall: London, 1973.

(12) Weller, A. *Prog. React. Kinet.* 1961, 1, 187–214.

(13) Birks, J. B. *Photophysics of Aromatic Molecules*; Wiley: New York, 1970.
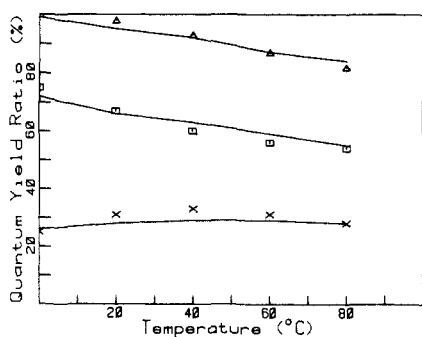
Figure 2. Quantum yield ratio vs. temperature at pH 2.96. Experimental data; ($\triangle$) $\Phi/\Phi_0 + \Phi'/\Phi_0'$, ($\square$) Φ/Φ_0, (X) Φ'/Φ_0', (solid lines) calculated from eq 7 and 8.

At the lower temperatures (0 and 20 °C), the temperature-dependent rates k_{dis}, k_{rec}, and k_s are relatively small and the (λ_1 + λ_2) plots are rather flat. Thus, the lower temperature data cannot yield very accurate values of the rate parameters. The accuracy becomes greater for the higher temperature data, so these points should be afforded more weight.

Both intercepts and slopes are seen to depend on temperature. This is in qualitative accord with the expected temperature dependence of k_{dis} and k_{rec}. In fact, the rate parameters obtained from the intercepts are in reasonable agreement with those reported earlier[6,8] from decay measurements on ROH*. The temperature-dependent intercepts fitted to $k_0 + k_0' + k_1^\circ \exp(-\Delta H^\ast_{dis}/k_B T)$, with k_B = Boltzmann's constant, give a prefactor k_1° of 7.5×10^9 s^{-1} and an activation barrier $\Delta H^\ast_{dis}$ of 2.6 kcal mol^{-1}, which are to be compared with 8.5×10^9 s^{-1} and 2.6 kcal mol^{-1} reported in ref 8.

While the intramolecular rate constants k_0 and k_0' are known[6] to be essentially temperature independent, simplifying the intercept analysis, a complication in the interpretation of the temperature-dependent slopes arises because of the unknown behavior of $k_q' + k_q$ with temperature. Because k_q is 2 orders of magnitude smaller than k_{rec} or k_q',[5] the slopes actually reflect only the quantity ($k_{rec} + k_q'$). In order to attempt a separation of k_{rec} and k_q' and to learn more about their temperature dependence, further information from quantum yield measurements is desirable.

Quantum Yields

From eq 3 and 4, one obtains

$$\frac{\Phi}{\Phi_0} = \frac{k_0 a'}{aa' - k_{dis}k_{rec}[H^+]} \tag{7}$$

$$\frac{\Phi'}{\Phi_0'} = \frac{k_0' k_{dis}}{aa' - k_{dis}k_{rec}[H^+]} \tag{8}$$

The denominators Φ_0 and Φ_0' on the left-hand sides of eq 7 and 8 are the *intramolecular* fluorescence quantum yields $k_r/(k_r + k_{nr})$ and $k_r'/(k_r' + k_{nr}')$, respectively, for [ROH*] and [RO*$^-$]. These intramolecular rates and quantum yields contain no contributions from k_{dis}, k_{rec}, k_q, or k_q' nor do they depend on pH or temperature over the experimental ranges covered.[4-7] The quantities Φ and Φ' are the fluorescence quantum yields in the presence of these other processes.

The quantum yield ratios Φ/Φ_0 and Φ'/Φ_0' for ROH* and RO*$^-$ at pH 2.96 together with their sum are plotted against temperature in Figure 2. Experimentally, Φ/Φ_0 is seen to decrease monotonically as the temperature increases, while Φ'/Φ_0' first increases and then apparently decreases slightly with increasing temperature, giving rise to a broad flat maximum between 20 and 60 °C. The behavior of Φ/Φ_0 is caused by the increase of k_{dis} with temperature, while that of Φ'/Φ_0' is a result of competetion among k_{dis}, k_{rec}, and k_q'.

The sum of the two quantum yield ratios tends to be below unity at high temperatures (Figure 2, top). Such a deviation is observed only at low pH and has been attributed to proton-induced quenching $k_q'[H^+]$.[5] At pH $\gtrsim$ 2.96, the increase of [H$^+$] from

0 to 80 °C is not more than 1–2%.[12,14] This is far too small to account for the observed ~20% drop of ($\Phi/\Phi_0 + \Phi'/\Phi_0'$) at the higher temperatures. Thus, it is suspected that k_q' itself is increasing as the temperature rises.

Discussion

In Table I, data calculated from the Arrhenius parameters[7] for the reference temperature of 298 K, at which no rate or quantum yield experiments were performed, have been included. In addition, we have listed dielectric relaxation times τ_d from Hasted's book[15] for each of the six temperatures. The Debye rotational correlation rate τ_D^{-1} of eq 1 and 2 is essentially proportional to τ_d^{-1} over the temperature range of interest.[16] The value of τ_d had to be interpolated for the 25 °C point and slightly extrapolated for the 80 °C point.

As mentioned earlier, the parameter k_q can be ignored compared with ($k_{rec} + k_q'$). It is believed that this feature provides a simplification in the analysis, since k_{rec} and k_q' represent parallel processes. The first parameter describes the rate at which a proton combines with RO*$^-$ to form the excited state of ROH, the second the rate at which a proton combines with RO*$^-$ to give the ground state of ROH. Thus, it would seem reasonable that k_{rec} and k_q' have identical temperature dependencies and that the sum k_s = ($k_{rec} + k_q'$) might behave in a manner given by eq 2.

The observed values of k_s in Table I are indeed approximately proportional to τ_d^{-1}, with a proportionality constant of 0.65 ± 0.04 for the more accurate data at the three higher temperatures. Application of this constant to τ_d^{-1} for all temperatures yields a set of "calculated" k_s, which are shown in column 5 of the table. The percentage errors for the data at 0 and 20 °C, as noted, are rather high, but the agreement over the entire range of temperatures 0–80 °C is generally acceptable.

If k_{rec} and k_q' have the same temperature dependence, then constant scale factors connect them with k_s. Using the absolute rate parameter k_{rec} (25 °C) = 58 ns^{-1} derived in previously work[8] shows that this scale factor is ~0.725 and is thus ~0.275 for k_q'. Values of k_{rec} and k_d' calculated with these scale factors for the six temperatures are given in columns 6 and 7 of Table I.

This analysis has shown that a set of rate parameters k_s = ($k_{rec} + k_q'$) exists, which fits the experimental lifetime data, where the temperature dependence of both k_{rec} and k_q' is the same as that of τ_D^{-1}, the Debye relaxation rate for pure liquid water. This finding is consistent with the rate equations proposed earlier[8] for weak, univalent acid dissociations and given for the special case of 2-naphthol as eq 1 and 2 of this paper.

One can now insert the values of k_{rec} and k_q', derived from the lifetime data, into eq 7 and 8 to verify that these temperature-dependent parameters also fit the experimental quantum yield data. Since the values of k_{rec} and k_q' in columns 6 and 7 of Table I and all other parameters needed are absolute values, there are no adjustable parameters in these fits. The results of this procedure are shown as the full lines in Figure 2. Again, the agreement, while not perfect, is acceptable.

Thus, the quantum yield data are also consistent with the idea that both k_{rec} and k_q' change with temperature as τ_D^{-1}. Other assumptions about the relationship between k_{rec} and k_q' are more arbitrary and fit the experimental data less well. For example, two limits can be assumed, one in which all the temperature dependence resides in k_{rec}, k_q' being totally independent of temperature, and the other limit where it all resides in k_q'. The inability of either of these assumptions to fit the quantum yield data is illustrated in Figure 3 for ($\Phi/\Phi_0 + \Phi'/\Phi_0'$). It is seen that these two theoretical curves lie on either side of, and are fairly far from, the experimental points.

Conclusions

By use of time-dependent and steady-state measurements, the proton dissociation and recombination rates and the proton-induced

(14) Harned, H. S.; Owen, B. B. *The Physical Chemistry of Electrolytic Solutions*, 3rd ed.; Reinhold: New York, 1958; p 466.

(15) Reference 11, Table 2.2, p 47.

(16) Reference 11, pp 21–22.

7480   *J. Am. Chem. Soc., Vol. 108, No. 24, 1986*

Lee et al.
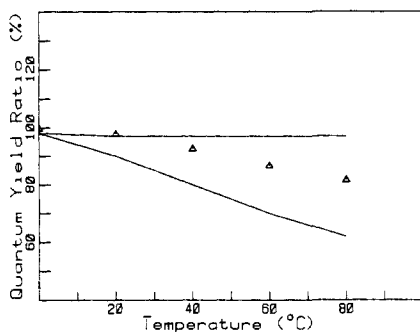
Figure 3. Summed quantum yield ratio vs. temperature at pH 2.96. Experimental data: ($\triangle$) $\Phi/\Phi_0 + \Phi'/\Phi_0'$ as in Figure 2, (solid lines) calculated from eq 7 and eq 8 but with parameters based on an analysis where k_q' is temperature independent (top) and where k_{rec} is temperature independent (bottom).

quenching rate for excited 2-naphthol are determined as a function of temperature. The rate parameter k_{dis} for proton dissociation is confirmed to be temperature dependent in the way found earlier from rate and quantum yield measurements on ROH alone. Within the rather wide range of data fitting errors, the evaluation of the rate parameter k_{rec} for the $H^+ + RO^{*-} \rightarrow ROH^*$ recombination is consistent with a picture where its temperature dependence is contained in $\Omega\tau_D^{-1}$ as given by eq 2. It is very likely that the parallel process, proton quenching of RO^{*-}, also has the temperature dependence of τ_D^{-1}. These findings support the weak acid proton hydration model presented earlier, which limits the ultrafast (<1 ps) longitudinal relaxation time to a non-rate-limiting role.[8] In fact the absolute values of k_{rec} throughout the entire range of experimental temperatures must be close to those given by eq 2 with $\Omega \approx 0.45$ and $\tau_D(T) \approx 0.95\tau_d(T)$.[7,8] Since the product $\Omega\tau_D^{-1}$ is the measured parameter, it is not possible from this type of experiment to obtain absolute values of Ω and τ_D separately.

The reader may be wondering at this point, "What's happened to the diffusion controlled rate for the recombination process?" Actually, because of *detailed balancing*,[17] a diffusion-controlled

rate in eq 2 under standard-state conditions (298 K, reactants at 1 M) has to be exactly equal to the $\Omega\tau_D^{-1}$ factor in k_{dis} of eq 1. This is possible since, quite accurately,[8,18] $\tau_D^{-1} = k_BT[AV_M\eta]^{-1}$ s^{-1}, where A is a temperature-independent dimensionless constant, $\eta = \eta(T)$ is the shear viscosity of liquid water, $V_M = V_M(T)$ is the molar volume of liquid water, and T is the absolute temperature. On the other hand, the diffusion-controlled recombination rate for ions in water (static permittivity $\epsilon \gg 1$) may be written[19] as $4\pi N_A r_0(D_+ + D_-) \div 1000$ M^{-1} s^{-1}, where N_A is Avogadro's number, r_0 is the "effective reaction distance", and $D_\pm$ are the diffusion coefficients of the ions. Conventional relationships between diffusion coefficients and shear viscosity have the form $D = k_BT/q\pi a\eta$, where q is a constant depending on the hydrodynamic boundary conditions ($q = 6$ for "sticking" boundary conditions) and a is the "radius" of the diffusing particle.[20] Thus, the diffusion-controlled rate is equal to $A'k_BT/\eta$, while the standard-state rate from eq 2 is equal to $A''k_BT/\eta$, and detailed balancing demands that $A' = A''$ at all experimental temperatures. These requirements of course run much deeper than the particular interpretation of any of the parameters in the rate expressions.

As a final word of warning, it is to be remembered that our data fitting analysis here and elsewhere[6-8] described k_{dis} as a simple Arrhenius rate. This is not really correct because neither τ_D^{-1} nor $exp[-\Delta G_i^\circ/RT]$ have Arrhenius behavior. The activation enthalpy for τ_D^{-1} decreases,[21] while for typical weak acids ΔG_i° increases with increasing temperature.[14] However, as explained in ref 8, a near cancellation of these effects occurs, providing a reasonably constant experimental ΔH^*_{dis} over the temperature range of interest.

Registry No. 2-Naphtholate, 15147-55-4.

(17) Fowler, R. H. *Statistical Mechanics*, 2nd ed.; Cambridge University Press: Cambridge, England, 1966; pp 659–660. Benson, S. W. *Thermochemical Kinetics*, 2nd ed.; Wiley: New York, 1975; p 14.

(18) Bassez, M.-P.; Lee, J.; Robinson, G. W., unpublished results.
(19) Debye, P. *Trans. Electrochem. Soc.* **1942**, *82*, 265. See also ref 10.
(20) Zwanzig, R. W.; Bixon, M. *Phys. Rev.* **1970**, *A2*, 2005–2012.
(21) Eisenberg, D.; Kauzmann, W. *The Structure and Properties of Water*; Oxford University Press: New York, 1969; Table 4.5, p 207.
(22) Webb, S. P.; Philips, L. A.; Yeh, S. W.; Tolbert, L. M.; Clark, J. H. *J. Phys. Chem.* **1986**, *90*, 5154.